THE JOURNAL OF PHYSICAL CHEMISTRY C

Article

pubs.acs.org/JPCC

A Reversible Molecular Switch Based on the Biphenyl Structure

Martin E. Zoloff Michoff,* M. Ezequiel Castillo, and Ezequiel P. M. Leiva

INFIQC, Departamento de Matemática y Física, Facultad de Ciencias Químicas, Universidad Nacional de Córdoba, Ciudad Universitaria, X5000HUA Córdoba, Argentina

Supporting Information

ABSTRACT: DFT calculations were performed on a biphenyl-based molecule bonded to gold nanoleads in order to evaluate its potential as a reversible molecular switch. The torsion angle (φ) between the aromatic rings may be controlled by means of reducing a disulfide functionality that bridges the two rings, giving rise to a "closed" species (disulfide bridge oxidized, $\varphi \sim 28°$) and an "opened" species (disulfide bridge reduced, $\varphi \sim 65°$). The mechanical properties of the nanojunction formed by this molecular species sandwiched between gold cluster pyramids mimicking metallic electrodes were determined. The thermodynamics of the reduction reaction was studied on the disulfide bridge as well as on the potentially competing anchoring sulfur atoms. A highly favorable product ratio toward the disulfide bridge reduction was found. Conductance values were calculated by means of non-equilibrium Green functions techniques. Interestingly, a significant difference between the closed (high conductance) and opened (low conductance) species was found.

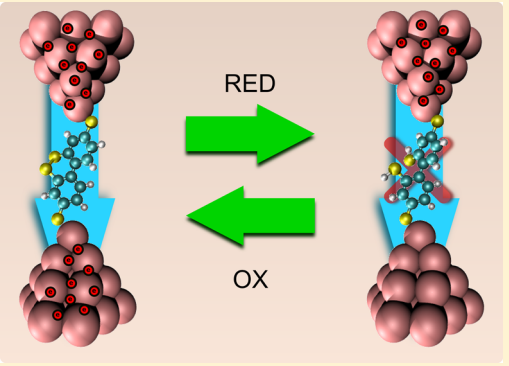

INTRODUCTION

Single-molecule junctions have attracted considerable attention from both an experimental and a theoretical point of view,[1−3] as they constitute the building blocks for a new paradigm in the fabrication of electronic devices known as "molecular electronics".[4] The fabrication of such molecular junctions, as well as understanding and controlling their properties, has become one of the major goals for scientists and engineers. Computational simulations have been shown to be an excellent tool, not only to provide insight into the underlying mechanisms of the making and breaking of such devices but also to contribute to the targeted design for a desired property.[5]

One of the main reasons that makes using single molecules in integrated circuits very attractive is that one can tailor the properties of the device by modifying a small portion of the building unit. The backbone of the molecule will ultimately determine the specific function of the molecular device. Many molecular structures with interesting electronic properties, such as poorly conducting wires (a resistance), highly conducting wires, diodes or rectifiers, and two- and three-terminal switches, have been identified.[3,6]

An interesting structure that has shown potential to be used as a molecular switch is the biphenyl. This molecule has attracted considerable interest as a model compound because of its size and the availability of numerous derivatives obtained by chemical modification. Its potential as a molecular switch is based on the fact that the two π systems can either be on the same plane or perpendicular to each other, thus representing the "on" and "off" states of a switch, respectively. This concept has been experimentally proved by Wandlowski and co-workers.[7−9] The conductance of a family of biphenyl molecules linked to two gold electrodes by means of a Au−S bond has been measured. In these experiments the torsion angle (φ) between the aromatic rings was fixed in each molecule by a CH_2 bridge of variable length. It was found that when twisting the biphenyl system from flat ($\varphi = 0°$) to perpendicular ($\varphi = 90°$) the conductance decreased by a factor of 30. Venkataraman et al. also found a similar behavior for biphenyl molecules with different ring substitutions that alter the twist angle of the molecules.[10] In this case the molecules were attached to gold electrodes through amine groups.

Some interesting open questions remain unanswered. How stable are these molecular contacts when subject to an external force? How could one modify the biphenyl structure to change the torsion angle with an external chemical or electrochemical signal and thus turn it into a reversible molecular switch? We will address these questions by means of a molecular structure based on the biphenyl motif with two thiol groups in 4,4′ positions for anchoring to the metallic electrodes and a disulfide bridge between 2,2′ positions (**SH-Ox**). The disulfide bond is prone to a reversible redox reaction that leads to a reduced species (**SH-Red**).

The molecule of interest is connected to two gold electrodes via Au−S bonds. In the oxidized form, the disulfide bridge holds the torsion angle at a fixed position, whereas when it is reduced this constraint is removed and the torsion angle can take a different value, which affects the transport properties of the system.

Received: May 13, 2013
Revised: October 23, 2013

   dx.doi.org/10.1021/jp4046963 | J. Phys. Chem. C XXXX, XXX, XXX−XXX

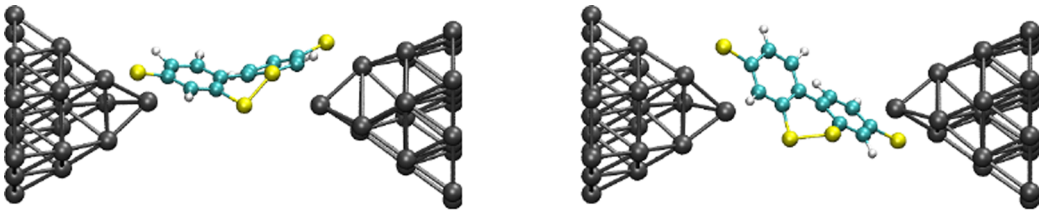

Figure 1. "*Cis*" and "*trans*" geometries considered when bonded to gold clusters.

We show that this system has the potential to constitute a reversible molecular switch. It should be noted that although this work does not deal with the kinetic aspects of the reduction−oxidation of the disulfide bridge in the target molecule, the reversibility of the switch could be achieved by means of appropriate electrochemical conditions to drive the reaction in one or the other direction.

METHODOLOGY

General. All calculations were performed using the DFT code SIESTA.[11] Exchange and correlation effects were taken into account using the generalized gradient approximation within the Perdew−Burke−Ernzerhof (PBE) functional.[12] Norm-conserving pseudopotentials (with relativistic corrections in the case of Au) generated according to the scheme of Troulliet and Martins[13,14] were used. The separation between the periodic images was maintained at 15 Å in all directions to ensure there was no interaction betweem them. The calculations were performed using the Γ point of the Brillouin zone and a double ζ basis set with polarization. Other relevant parameters for the quality of the calculations are the energy shift used to confine the electrons in the pseudoatomic orbitals (0.01 eV) and the energy cutoff that defines the grid used to represent the charge density (200 Ry). We took care to test convergence of our results with respect to all these parameters. Geometry optimizations were performed using the conjugate gradient (CG) algorithm until a maximum force of 0.01 eV Å^{-1} was reached.

Initial Structures and Mechanical Stretching of the Molecular Junction. The initial structures were built on the assumption that the molecular wires are formed using the "STM/AFM−break junction" technique as implemented by Tao and co-workers,[15] Venkataraman and co-workers,[16] and Wandlowski and co-workers.[17] Initially, a mechanical contact is established between the tip and the surface (both Au). Upon retraction, a metallic neck bridges the gap between the tip and the surface, which at some point turns into a monatomic metallic wire identified by its characteristic signature of 1 G_0 conductance (where $G_0 = 2e^2/h = 7.748 \times 10^{-5}\ \Omega^{-1}$ is the quantized unit of electrical conductance). When the external stress reaches the breaking point for the gold wire, the molecules establish a bridge between the tip and the surface. Experimental and theoretical work has shown that the monatomic Au wire can be of up to 4 atoms long.[18,19] The maximum stretching for such a wire leads to a structure in which the Au−Au distance is 2.88 Å,[20] leaving a gap of ∼8.6 Å. This is the initial point for our simulations, in which we model the molecular junction formed by a 4,4′-biphenyl dithiol with a disulfide bridge between the 2 and 2′ atoms (**SH-Ox**) using two 23-atom clusters as contacts. The Au pyramids were obtained from a Au(111) slab by taking 12, 7, and 3 atoms from consecutive layers. The atom in the apex of the pyramid was placed at an adatom site. We have considered two different possible geometries for the **SH-Ox** molecule bonded to the Au clusters that we have called "*cis*" (**Au-S-Ox-cis**) and "*trans*" (**Au-S-Ox-trans**). In the "*cis*" geometry, both terminal thiol groups are appended to the gold clusters on the same side, whereas in the "*trans*" geometry, the thiol groups are appended on opposite sides of the gold clusters. These are illustrated in Figure 1.

We are aware that competition between 4,4′ and 2,2′ sulfur atoms for binding to gold electrodes is likely to exist. This would certainly lead to different junctions with different properties than those studied here. Nonetheless, using the appropriate experimental conditions it should be possible to minimize this competition, as has been shown to be the case for the adsorption of cysteine and cystine on Au(111).[21]

To relieve the stress of the molecular junction that might arise from the particular choice of the initial geometries, we performed a stretching of the molecular nanojunction. A COGEF (constrained geometries simulate an external force) approach was used to model the external pulling force of an AFM tip.[22] This was accomplished by constraining the most external planes of gold atoms in each cluster to be fixed at their bulk positions. The distance between these two planes was increased in a stepwise fashion in increments of 0.1 Å, and the entire system was allowed to relax at each step with the aforementioned constraints. This procedure was continued until the rupture of the molecular junction was observed. This allowed us to determine the mechanical properties of the nanojuctions, which were evaluated from the binding energies, E_b, and rupture forces, F_{rup}, obtained from an energy profile upon stretching of the nanojuntion. The energy profiles were fitted with an appropriate Chevyshev polynomial. The force at each point was obtained as the derivative of the fitted energy curve.

Reduction Reactions. The thermodynamics of the reduction reactions on both sulfur sites (anchoring and disulfide bridge) were studied. The first minima from the stretching energy profiles for the oxidized species (**Au-S-Ox** "*cis*" and "*trans*") were taken, and hydrogen atoms were added at suitable positions close to the sulfur atoms of either the anchoring sites or the disulfide bridge. Geometry optimization with the aforementioned constraints was performed for each structure. This procedure emulates an electrochemical reduction process in which potential control would allow the controlled reduction of the molecules.

Conductance Calculations. The current flowing through the molecule coupled to two electron reservoirs (leads) was calculated by means of an in-house code based on the non-equilibrium Green function operator (NEGFC).[23] The details about the implementation of the code and its use to calculate

dx.doi.org/10.1021/jp4046963 | J. Phys. Chem. C XXXX, XXX, XXX−XXX

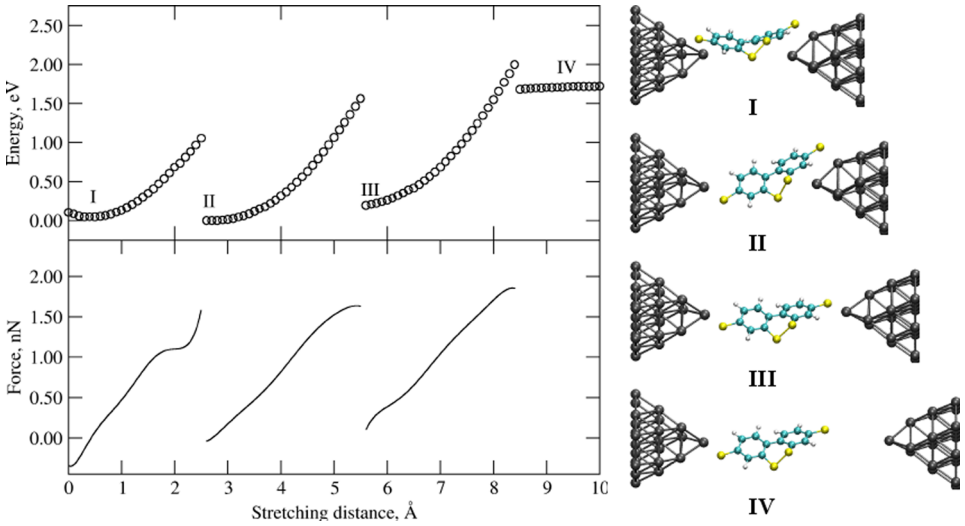

Figure 2. Mechanochemical behavior of **Au-S-Ox-cis**. Left panel: Energy and force profiles for the stretching of the nanojunction. Right panel: Selected structures along the stretching simulation.

the transport properties of 1,8-octanedithiol sandwiched between a gold surface and a gold tip can be found elsewhere.[24] In this work the electronic structure of selected configurations along the stretching profiles were determined using the SIESTA Hamiltonian. All "s", "p", and "d" pseudo orbitals for Au are considered to be equally coupled to the leads through the parameter γ. In the present work a total of 24 leads were used to contact the Au atoms laying in the outermost planes of the clusters. The fitting procedure for the γ parameter, as described in ref 24, was used, yielding a value of −2.82 eV, which was used throughout the calculations (refer to Figures S1 and S2 in the Supporting Information).

RESULTS

Mechanical Stretching of the Molecular Junction. "*Cis*" and "*trans*" geometries gave identical results with respect to the energy profile while stretching the nanojunction. The typical mechanochemical behavior of these systems is illustrated in the upper plot in the left panel of Figure 2. A sawtoothlike curve with three well-defined minima along the stretching curve is observed. At the final stage, the rupture of the nanojunctions occurs at a S−Au bond.

Bonding energies (E_b) and rupture forces (F_{rup}) obtained from the energy profiles are summarized in Table 1. E_b values are defined as the energy difference between the minimum structure for the step that leads to the breakage of the nanojunction and the "broken" structure. Likewise, the F_{rup} values are obtained as the maximum value from the force profile for the rupture step.

Table 1. Mechanical Properties of the Systems Studied in This Work Characterized by Their Bonding Energies (E_b) and Rupture Forces (F_{rup})

system	E_b (eV)	F_{rup} (nN)
Au-S-Ox-cis	1.53[a]	1.86[b]
Au-S-Ox-trans	1.50[a]	1.94[b]

[a]Taken as the energy difference between structures **III** and **IV** as illustrated in Figure 2. [b]Maximum value along the stretching simulation between structures **III** and **IV** as illustrated in Figure 2.

Reduction Reactions. The reduction of the disulfide bridge would allow us to modify the torsion angle between the aromatic rings in the biphenyl structure, and thus it would have an impact on the transport properties of the molecular wire. The thermodynamics of this reaction was studied along with its competing, and in principle undesirable, side reaction which is the reduction of the anchoring sulfur atoms.

The corresponding energy changes, ΔU_{red}, for the reduction of the structure corresponding to the first energy minimum encountered along the stretching of **Au-S-Ox** "*cis*" and "*trans*" were calculated as given by eq 1, where **R** is the fully oxidized species and $\mathbf{P_T}$ and $\mathbf{P_B}$ are the products that result from reducing the terminal or anchoring sulfur atoms and the disulfide bridge, respectively. This is illustrated in Figure 3. The corresponding reduction potentials, E_{red}, were then approximated according to eq 2, where n is the number of electrons transferred in the reaction (n = 2 for the reations studied here) and e is the charge of an electron. The calculated E_{red} values are relative to the standard hydrogen electrode (SHE). Table 2 summarizes the calculated values for ΔU_{red} and E_{red}.

$$\Delta U_{red} = E(\mathbf{P_T} \text{ or } \mathbf{P_B}) - E(\mathbf{R}) - E(H_2) \quad (1)$$

$$E_{red} = -\Delta U_{red}/ne \quad (2)$$

Conductance Calculations. Conductance values at zero bias were calculated for the first energy minimum along the stretching simulations for **Au-S-Ox** "*cis*" and "*trans*" as well as for the reduced products on the disulfide bridge and on the anchoring sulfur atoms. The results are summarized in Table 3.

DISCUSSION

Electronic Structure and Bonding. The results obtained from the stretching of the molecular nanojunctions show that the proposed system has mechanical properties similar to those of other thiolate−gold nanojunctions. Bonding energies of ∼1.5 eV for thiolate-bonded systems are in good agreement with calculated values for thiol and thiolate adsorption on Au(111).[25−30] Rupture forces of ∼1.9 nN are also in excellent agreement with other calculated values from isotensional stretching of a octanedithiol/ate−gold nanojunction.[31,32]

A detailed account of the mechanochemical properties of this system and for similar systems in which the molecule is subject

dx.doi.org/10.1021/jp4046963 | J. Phys. Chem. C XXXX, XXX, XXX−XXX

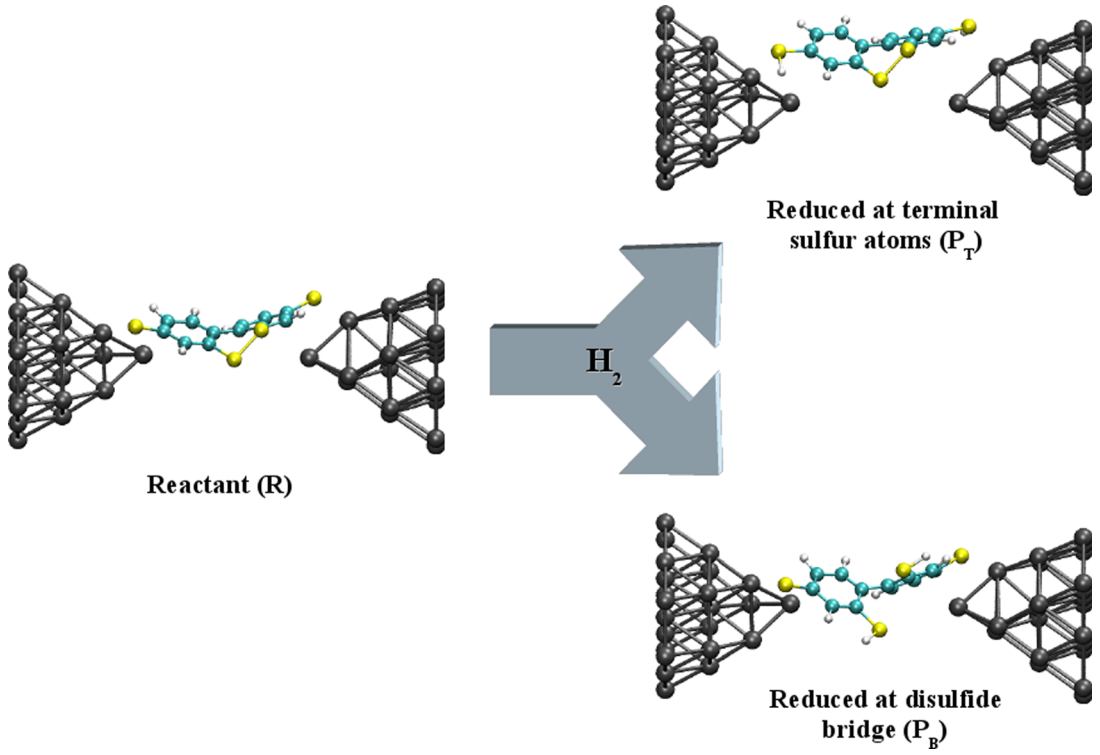

Figure 3. Illustrative example for the reactant and products of the reduction of sulfur atoms in the **Au-S-Ox-cis** system stretched at 0.4 Å.

Table 2. Thermodynamic Quantities for the Reduction of Bridge and Anchoring Sulfur Atoms of Au-S-Ox-cis and Au-S-Ox-trans and Reduction Potentials Relative to the SHE for These Reactions

ΔU_{red} (bridge) (eV)	ΔU_{red} (terminal) (eV)	E_{red} (bridge) vs HRE (V)	E_{red} (terminal) vs HRE (V)	E_{red} (bridge) − E_{red} (terminal) (V)
		Au-S-Ox-cis[a]		
−0.426	0.163	+0.213	−0.082	0.295
		Au-S-Ox-trans[b]		
−0.384	0.266	+0.192	−0.133	0.325

[a]Structure for the reactant taken from the stretching path at 0.4 Å. [b]Structure for the reactant taken from the stretching path at 0.2 Å.

Table 3. Conductance Values in Units of G_0 and Dihedral Angle between the Aromatic Rings for Au-S-Ox, Au-S-Red, and Au-SH-Ox "*cis*" and "*trans*"

reactant (R)		reduced at disulfide bridge (P_B)		Reduced at terminal sulfur atoms (P_T)	
dihedral angle (deg)	G/G_0	dihedral angle (deg)	G/G_0	dihedral angle (deg)	G/G_0
		Au-S-Ox-cis[a]			
25.5	0.046	54.7	0.021	32.3	0.0025
		Au-S-Ox-trans[b]			
33.5	0.042	68.1	0.0063	30.8	0.0081

[a]Structure for the reactant taken from the stretching path at 0.4 Å. [b]Structure for the reactant taken from the stretching path at 0.2 Å.

to different degrees of reduction on the sulfur atoms will be the subject of a future contribution. For the purpose of this work, we will now focus on the first minimum encountered along the stretching profile (structures labeled as **I** in Figure 2 for **Au-S-Ox-cis** and in Figure S3 of the Supporting Information for **Au-S-Ox-trans**).

To gain insight into the nature of the chemical bonding of the molecule to the gold clusters, we performed an analysis of the charge density difference between the **Au-S-Ox** "*cis*" and "*trans*" systems and the combined isolated Au clusters and molecular radicals. Figure 4 shows the calculated isosurface for

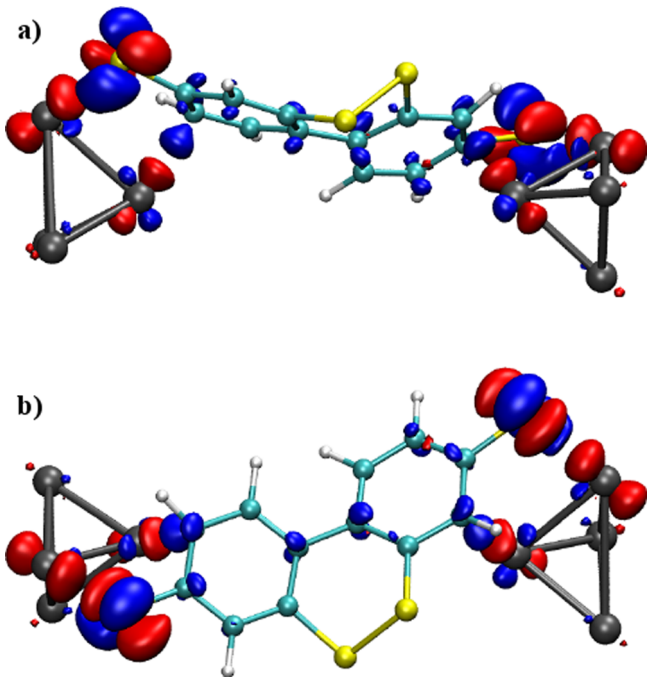

Figure 4. Calculated isosurface (at an isovalue of 0.005 e bohr^{-3}) for the differential charge density of **Au-S-Ox-cis**. Top and bottom panels show two different views. Blue indicates a positive value (i.e., charge accumulation) and red indicates a negative value (i.e., charge depletion).

dx.doi.org/10.1021/jp4046963 | J. Phys. Chem. C XXXX, XXX, XXX−XXX

Table 4. Mulliken Population Analysis on the Sulfur Atoms, Charge Transferred from Gold Clusters to the Molecule and Mulliken Overlap Population Analysis for Au−C and Au−S Interactions for Au-S-Ox "*cis*" ans "*trans*" (R) and Their Respective Reduction Products on the Sulfur Terminal Atoms (P_T) and on the Disulfide Bridge (P_B)

	E_{frag} (eV)[a]	Δ charge (*e* Au/molecule)[b]	S terminal population[c]	S bridge population[d]	MOP Au−S[e]	MOP Au−C[f]
			Au-S-Ox-cis			
R	−2.00	+0.37/−0.37	6.32	6.12	0.22	0.10
P_T	−0.36	−0.24/+0.24	5.94	6.11	0.09	0.00
P_B	−2.08	+0.32/−0.32	6.34	5.92	0.20	0.10
			Au-S-Ox-trans			
R	−2.12	+0.35/−0.35	6.34	6.12	0.22	0.11
P_T	−0.46	−0.28/+0.28	5.93	6.11	0.06	0.05
P_B	−2.24	+0.33/−0.33	6.35	5.93	0.22	0.11

[a]Calculated as the energy difference between the optimized molecular junction and the combined fragments, gold clusters, and isolated molecule without further relaxation. [b]Obtained by summing up the Mulliken charges for the gold clusters and molecule respectively. [c]Average value for terminal S atoms. [d]Average value for S atoms in disulfide bridge. [e]Obtained by summing up the MOP values between the terminal sulfur atoms and all Au atoms in the cluster to which it is bonded. The values reported are the average for both terminal sulfur atoms in the molecule. [f]Obtained by summing up the MOP values between the carbon atoms in each ring and all Au atoms in the nearest cluster. The values reported are the average for both aromatic rings.

Au-S-Ox-cis as an illustrative example (refer to Figure S4 in the Supporting Information for the corresponding isosurface for **Au-S-Ox-trans**). As can be observed, charge transfer occurs from the gold clusters to the molecule. Mulliken population analyses show that ∼0.4 *e* is being transferred (see Table 4), where *e* is the magnitude of the charge of an electron. Changes of ca. 0.2 *e* have been reported for experimental studies on thiol chemisorption.[33−35] DFT calculations have also shown that a charge transfer of ∼0.14−0.17 *e* is typically transferred from the surface to the molecule in the case of alkyl thiolates adsorbed on Au(111) surfaces.[36,37]

As can be gathered from Figure 4, the charge density gain is partially transferred from the anchoring sulfur to the carbon backbone. This takes place through extended conjugation of 3p S orbitals with the π system of the ring. This is demonstrated by examining the projected DOS for the 3p orbitals of the anchoring sulfur atoms and the 2p orbitals of the carbon atoms to which they are directly bonded. Figure 5 illustrates this bonding situation, where it can be observed that the PDOS of S 3p shares some peaks in common with both Au 5d and C 2p orbitals.

Another interesting feature that emerges from the differential charge density analysis illustrated in Figure 4 is that there is a bonding interaction between the Au atoms in the apex of each cluster with a carbon atom in each aromatic ring of the molecule. This interaction was quantified by means of the Mulliken overlap population (MOP) analysis,[38] and the corresponding values are summarized in Table 4 as MOP Au−C. For comparison, MOP values for the interaction between the terminal sulfur atoms and the gold clusters are also summarized in Table 4.

Bonding interactions between Au and C are not as common as Au−S interactions in nanojunctions, but they are not unprecedented. Molecular species with an isocyanide functionality have been shown to bind to metallic surfaces through a C−M bond[39] and even yield stable single-molecule junctions with gold electrodes.[40,41] Direct bonding of aromatic or aliphatic hydrocarbons to gold, and its transport properties, has been studied from a theoretical point of view for some time,[42−45] but it was not until recently that highly conducting single-molecule junctions through direct Au−C contacts have been achieved experimentally.[46,47] Hydrocarbons can also interact with metallic surfaces through weaker van der Waals

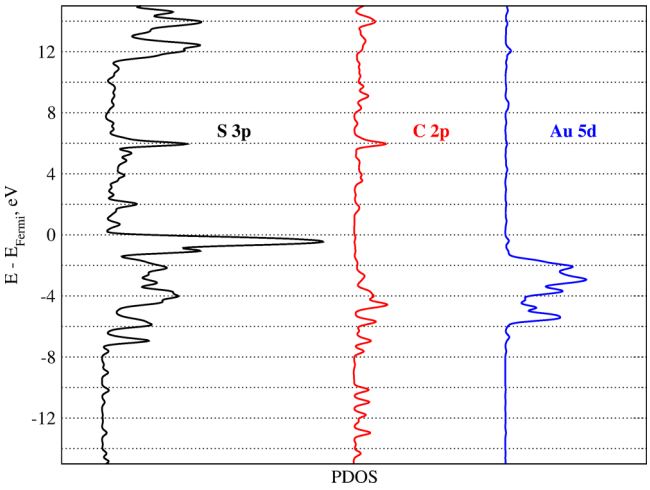

Figure 5. PDOS analysis for **Au-S-Ox-cis**: (black) 3p orbital for S terminal, (red) 2p orbital for C atom directly bonded to the terminal S, and (blue) 5d orbital of Au directly bonded to the terminal S. The PDOS curves corresponding to the C 2p and Au 5d orbitals have been shifted in the horizontal axis for the sake of clarity.

interactions. This has been shown to be the case for polycyclic aromatic hydrocarbons adsorbed onto a Au(111) surface by means of DFT calculations employing semiempirical corrections or a first-principles vdW-DF functional.[48] Nonspecific van der Waals interactions between the molecule's backbone and the gold electrodes have been shown to play a key role in the junction mechanics and its transport properties.[49,50]

Reduction Reactions. As was noted in the case of their mechanical properties, no substantial differences between "*cis*" and "*trans*" configurations are predicted concerning their behavior toward the reduction of the different sulfur sites. Notably, the reduction on the disulfide bridge is more favorable than that of the anchoring sulfur atoms. This is the desired behavior for the application of the molecular wire as a switch. Notice that the difference in reduction potential for both reduction reactions is ∼0.30 V. This turns into a 10^{10} fold ratio between equilibrium constants at room temperature, making it possible to reduce selectively the disulfide bridge by choosing adequate experimental conditions.

This difference in reactivity can be understood in terms of the electronic structure analysis described above. The reduction

dx.doi.org/10.1021/jp4046963 | J. Phys. Chem. C XXXX, XXX, XXX−XXX

of the terminal sulfur atoms implies that conjugation between the 3p orbitals in the sulfur and the 2p orbitals in the adjacent carbon is no longer possible. Although a similar interaction is present for the disulfide bridge atoms with their adjacent carbon atoms, their reduction does not break this interaction because the disulfide bond is simultaneously broken. The reduction of the terminal sulfur atoms partially hinders charge transfer between the gold clusters and the molecule. As can be gathered from the information provided in Table 4, the magnitude of the charge transfer is diminished for the reduction product on the terminal sulfur atoms with respect to the reactant and the reduction product on the disulfide bridge. Also, there is an inversion in the sense of charge transfer, i.e., for $\mathbf{P_T}$, electrons flow from the molecule to the clusters, whereas for **R** and $\mathbf{P_B}$, electrons flow from the cluster to the molecule upon bonding. This bonding picture is supported by the differential charge density analysis (refer to Figure 4 and Figures S5 and S6 in the Supporting Information).

Finally, the bonding Au−C interaction is lost upon reduction of the sulfur terminal atoms. This is not the case for the reduction of the disulfide bridge (compare the Au−C MOP values in Table 4). This a consequence of a longer Au−S bond for $\mathbf{P_T}$ (∼2.60 Å) with respect to **R** and $\mathbf{P_B}$ (∼2.40 Å).

All these effects add up to weaker bonding between the molecule and the gold clusters when reduction at the terminal sulfur atoms have taken place, which becomes evident by comparing the fragmentation energies (E_{frag}) summarized in Table 4, leading to a product that is less stable than the reduction at the disulfide bridge.

Transport Properties. It is worth noting that the calculated values are in very good qualitative agreement with those calculated by Mishchenko et al. for a series of biphenyl structures with a variable length $-CH_2-$ bridge joining the aromatic rings.[7,9]

As can be observed from the values reported in Table 3, the conductance ratio between the oxidized species, which represents the closed state in the molecular switch, is ∼2-fold for the "*cis*" geometry and ∼6-fold for the "*trans*" geometry higher that the corresponding opened species ($\mathbf{P_B}$). The structure reduced on the sulfur anchoring atoms shows an even greater decrease in conductance. A similar decrease in conductance at low bias values upon protonation of the sulfur atoms has been reported for the thiophenol−Au nanojuntion.[51]

To gain further insight into how the electronic structure of the nanojunction influences the transport properties, we examined the transmission curves for the different species. Figure 6 shows the corresponding transmission curves for the **Au-S-Ox-cis** system in its oxidized form and for the reduction products $\mathbf{P_B}$ and $\mathbf{P_T}$. As can be observed, the transport properties for the closed (Figure 6a) and opened (Figure 6b) species are dominated by the highest occupied molecular orbital (HOMO) level. Figure 7 shows the calculated isosurface for these molecular orbitals, which display a π symmetry. These results are consistent with those found for other biphenyl molecules bonded to Au metallic tips by means of a Au−S bond.[7,9] In these experimental and theoretical works the torsion angle between the aromatic rings was fixed and controlled by means of either a variable length methylene bridge or the steric effect exerted by methyl groups at the 2,2′ positions. Our findings reported in this work indicate that the same *off-resonant* charge transport dominated by a $\pi-\pi$ coupling mechanism operates for our proposed molecular structure.

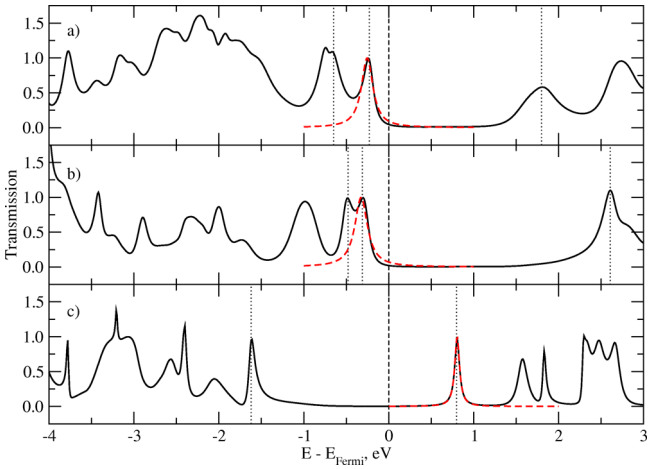

Figure 6. Transmission as a function of energy for **Au-S-Ox-cis**. The vertical dashed line indicates the Fermi level (set at zero), whereas the vertical dotted lines indicate the position of the HOMO (at negative energies) and the LUMO (at positive energies). The dashed red curves are the fitting of the resonance peak closest to the Fermi level to eq 3. (a) Oxidized species. (b) Reduced species at the disulfide bridge. (c) Species reduced at the terminal sulfur atoms.

As can also be gathered from Figure 6, the higher conductance of the closed species with respect to the opened one can be attributed to the HOMO level being closer to the Fermi level of the nanojunction (refer to the values summarized in the second column in Table 5). As for the biphenyl molecules studied by Mishchenko et al.,[7] a splitting of the HOMO into symmetrical and antisymmetrical orbitals is observed. As was also noted in that work, this splitting is reduced with the increasing of the torsion angle between the rings. At the limiting case for $\varphi = 90°$, these two energy levels are degenerate.

On the other hand, the transport properties of the species reduced at the terminal sulfur atoms is dominated by the lowest unoccupied molecular orbital (LUMO), and its lower conductance can be attributed to the combination of two effects: on one side, the LUMO orbital is at even higher energies from the Fermi level and, on the other side, to a weaker coupling of the molecule to the metallic leads as can be inferred from the width of the dominating peak in the transmission curve shown in Figure 6c. In order to quantify, at least in an approximate way, this difference in coupling of the molecule to the gold leads, we fitted the resonance of the transmission curves closer to the Fermi level to a simple Lorentzian model (eq 3).[52] This model is characterized by the energy of orbital (ε_0) responsible for the transmission peak and the coupling of the molecule to the metallic leads (we have assumed a symmetrical junction and hence the coupling to both leads is equal to Γ). The parameters obtained from the fitting procedure are summarized in Table 5.

$$T(E) = \frac{\Gamma^2/4}{(E - \varepsilon_0)^2 + \Gamma^2/4} \quad (3)$$

The Γ values obtained for our system are in good qualitative agreement with those reported for other biphenyl systems[9] and for benzene dithiol bonded to gold leads.[52] Nevertheless, these values should be regarded only as approximate measures of the coupling constants. Indeed, the high Γ value obtained for the reduced product at the terminal sulfur atoms for the "*trans*"

dx.doi.org/10.1021/jp4046963 | J. Phys. Chem. C XXXX, XXX, XXX−XXX

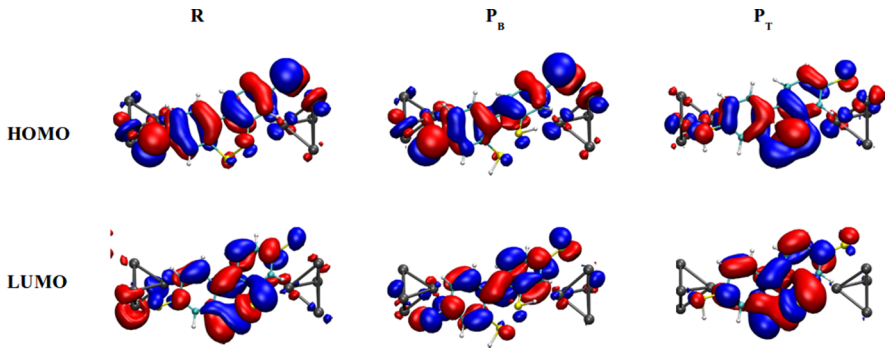

Figure 7. Calculated isosurfaces (0.05 e/Å^3) for the HOMO and LUMO orbitals for the **Au-S-Ox-cis** system and the reduction products. For the oxidized species (**R**) and the products of reducing the disulfide bridge, only the antisymmetrical orbital is shown.

Table 5. Energies of the HOMO and LUMO Orbitals and Parameters ε_0 and Γ Obtained by Fitting the DFT-Based Transmission Curves to the Lorentzian Model for Au-S-Ox "*cis*" ans "*trans*" and Their Respective Reduction Products

	$\varepsilon_{HOMO} - E_{Fermi}$ (eV)[a]	$\varepsilon_{LUMO} - E_{Fermi}$ (eV)	$\varepsilon_0 - E_{Fermi}$ (eV)	Γ (eV)
		Au-S-Ox-cis		
R	−0.65/−0.23	+1.82	−0.25	0.16
$\mathbf{P_B}$	−0.48/−0.30	+2.61	−0.32	0.18
$\mathbf{P_T}$	−1.61	+0.81	+0.81	0.07
		Au-S-Ox-trans		
R	−0.63/−0.22	+1.74	−0.27	0.16
$\mathbf{P_B}$	−0.36/−0.32	+1.81	−0.35	0.18
$\mathbf{P_T}$	−1.81	+0.49	+0.55	0.28

[a]For species **R** and $\mathbf{P_B}$, the two values reported are the symmetrical (left) and asymmetrical (right) orbitals for the HOMO doublet.

geometry can be related to more than one orbital contributing to the dominating transmission peak, and hence the use of a single-level model might not be justified in this case (see Figure S7 in the Supporting Information).

In summary, all these data show that our proposed molecular switch displays transport properties similar to those of other biphenyl systems studied from an experimental and a theoretical point of view.

CONCLUSIONS

In this work we have shown that the system proposed has the potential to work as a reversible molecular switch. It presents adequate mechanical properties when bonded to gold electrodes, and it would be possible to adjust the conditions to reduce the switching functionality without affecting the anchoring groups. The ratio between high and low conducting species is ∼2−6 times. Although this is an entirely theoretical work, we hope that it could serve as an inspiration for experimentalist groups to design experiments to test these findings.

ASSOCIATED CONTENT

Supporting Information

Fitting procedure for the γ parameter used in NEGFC calculations (Figures S1 and S2), energy and force profiles for **Au-S-Ox-trans** (Figure S3), differential charge density analysis for **Au-S-Ox-trans** and the reduction products of **Au-S-Ox-cis** (Figures S4−S6), and transmission curves for **Au-S-Ox-trans** and its reduction products (Figure S7). This material is available free of charge via the Internet at http://pubs.acs.org.

AUTHOR INFORMATION

Corresponding Author

*Edificio Integrador−Subsuelo, Haya de la Torre y Medina Allende, Ciudad Universitaria, X5000HUA Córdoba, Argentina. E-mail: martinz@fcq.unc.edu.ar. Tel/fax: +54 351 5353853.

Notes

The authors declare no competing financial interest.

ACKNOWLEDGMENTS

The authors acknowledge CONICET PIP: 112-200801-000983 and PIP 11220110100992, Secyt (Universidad Nacional de Córdoba, Argentina), Program BID (PICT 2012-2324), and PME: 2006-01581 for financial support. M.E.C. is a grateful recipient of a Ph.D. scholarship from CONICET. The authors also gratefully acknowledge Dr. Christian F. A. Negre for providing the first version of the homebuilt NEGFC code.

REFERENCES

(1) Kiguchi, M.; Kaneko, S. Single Molecule Bridging Between Metal Electrodes. *Phys. Chem. Chem. Phys.* **2013**, *15*, 2253−2267.

(2) Chen, F.; Hihath, J.; Huang, Z.; Li, X.; Tao, N. J. Measurement of Single-Molecule Conductance. *Annu. Rev. Phys. Chem.* **2007**, *58*, 535−564.

(3) Tao, N. J. Electron Transport in Molecular Junctions. *Nat. Nanotechnol.* **2006**, *1*, 173−181.

(4) Ratner, M. A. Introducing Molecular Electronics. *Mater. Today* **2002**, *5*, 20−27.

(5) Zoloff Michoff, M. E.; Vélez, P.; Dassie, S. A.; Leiva, E. P. M. Computational Tools to Study and Predict the Long-Term Stability of Nanowires. In *Electrodeposited Nanowires and their Applications*; Lupu, N., Ed.; InTech: Vukovar, Croatia, 2010; pp 1−34.

(6) Li, C.; Mishchenko, A.; Wandlowski, T. Charge Transport in Single Molecular Junctions at the Solid/Liquid Interface. In *Unimolecular and Supramolecular Electronics II*; Metzger, R. M., Ed.; Topics in Current Chemistry; Springer: Berlin/Heidelberg, 2012; Vol. *313*, pp 121−188.

(7) Mishchenko, A.; Vonlanthen, D.; Meded, V.; Bürkle, M.; Li, C.; Pobelov, I. V.; Bagrets, A.; Viljas, J. K.; Pauly, F.; Evers, F.; et al. Influence of Conformation on Conductance of Biphenyl-Dithiol Single-Molecule Contacts. *Nano Lett.* **2010**, *10*, 156−163.

(8) Vonlanthen, D.; Mishchenko, A.; Elbing, M.; Neuburger, M.; Wandlowski, T.; Mayor, M. Chemically Controlled Conductivity: Torsion-Angle Dependence in a Single-Molecule Biphenyldithiol Junction. *Angew. Chem., Int. Ed.* **2009**, *48*, 8886−8890.

(9) Bürkle, M.; Viljas, J. K.; Vonlanthen, D.; Mishchenko, A.; Schön, G.; Mayor, M.; Wandlowski, T.; Pauly, F. Conduction Mechanisms in Biphenyl Dithiol Single-Molecule Junctions. *Phys. Rev. B: Condens. Matter Mater. Phys.* **2012**, *85*, 075417.

(10) Venkataraman, L.; Klare, J. E.; Nuckolls, C.; Hybertsen, M. S.; Steigerwald, M. L. Dependence of Single-Molecule Junction

Conductance on Molecular Conformation. *Nature* **2006**, *442*, 904−907.
(11) Artacho, E.; Anglada, E.; Diéguez, O.; Gale, J. D.; García, A.; Junquera, J.; Martin, R. M.; Ordejón, P.; Pruneda, J. M.; Sánchez-Portal, D.; et al. The SIESTA Method: Developments and Applicability. *J. Phys.: Condens. Matter* **2008**, *20*, 064208.
(12) Perdew, J. P.; Burke, K.; Ernzerhof, M. Generalized Gradient Approximation Made Simple. *Phys. Rev. Lett.* **1996**, *77*, 3865−3868.
(13) Troullier, N.; Martins, J. L. Efficient Pseudopotentials for Plane-Wave Calculations. *Phys. Rev. B: Condens. Matter Mater. Phys.* **1991**, *43*, 1993−2006.
(14) Troullier, N.; Martins, J. L. Efficient Pseudopotentials for Plane-Wave Calculations. II. Operators for Fast Iterative Diagonalization. *Phys. Rev. B: Condens. Matter Mater. Phys.* **1991**, *43*, 8861−8869.
(15) Xu, B.; Tao, N. J. Measurement of Single-Molecule Resistance by Repeated Formation of Molecular Junctions. *Science* **2003**, *301*, 1221−1223.
(16) Venkataraman, L.; Klare, J. E.; Tam, I. W.; Nuckolls, C.; Hybertsen, M. S.; Steigerwald, M. L. Single-Molecule Circuits with Well-Defined Molecular Conductance. *Nano Lett.* **2006**, *6*, 458−462.
(17) Pobelov, I. V.; Mészáros, G.; Yoshida, K.; Mishchenko, A.; Gulcur, M.; Bryce, M. R.; Wandlowski, T. An Approach to Measure Electromechanical Properties of Atomic and Molecular Junctions. *J. Phys.: Condens. Matter* **2012**, *24*, 164210.
(18) Rubio-Bollinger, G.; Bahn, S. R.; Agraït, N.; Jacobsen, K. W.; Vieira, S. Mechanical Properties and Formation Mechanisms of a Wire of Single Gold Atoms. *Phys. Rev. Lett.* **2001**, *87*, 026101.
(19) Huang, F.; Chen, F.; Bennett, P. A.; Tao, N. J. Single Molecule Junctions Formed via Au−Thiol Contact: Stability and Breakdown Mechanism. *J. Am. Chem. Soc.* **2007**, *129*, 13225−13231.
(20) Vélez, P.; Dassie, S. A.; Leiva, E. P. M. When Do Nanowires Break? A Model for the Theoretical Study of the Long-term Stability of Monoatomic Nanowires. *Chem. Phys. Lett.* **2008**, *460*, 261−265.
(21) Hager, G.; Brolo, A. G. Adsorption/desorption Behaviour of Cysteine and Cystine in Neutral and Basic Media: Electrochemical Evidence for Differing Thiol and Disulfide Adsorption to a Au(111) Single Crystal Electrode. *J. Electroanal. Chem.* **2003**, *550*−*551*, 291−301.
(22) Ribas-Arino, J.; Marx, D. Covalent Mechanochemistry: Theoretical Concepts and Computational Tools with Applications to Molecular Nanomechanics. *Chem. Rev.* **2012**, *112*, 5412−5487.
(23) Xue, Y.; Datta, S.; Ratner, M. A. Charge Transfer and "Band Lineup" in Molecular Electronic Devices: A Chemical and Numerical Interpretation. *J. Chem. Phys.* **2001**, *115*, 4292−4299.
(24) Paz, S. A.; Zoloff Michoff, M. E.; Negre, C. F. A.; Olmos-Asar, J. A.; Mariscal, M. M.; Sánchez, C. G.; Leiva, E. P. M. Configurational Behavior and Conductance of Alkanedithiol Molecular Wires from Accelerated Dynamics Simulations. *J. Chem. Theory Comput.* **2012**, *8*, 4539−4545.
(25) Pensa, E.; Cortés, E.; Corthey, G.; Carro, P.; Vericat, C.; Fonticelli, M. H.; Benítez, G.; Rubert, A. A.; Salvarezza, R. C. The Chemistry of the Sulfur−Gold Interface: In Search of a Unified Model. *Acc. Chem. Res.* **2012**, *45*, 1183−1192.
(26) Askerka, M.; Pichugina, D.; Kuz'menko, N.; Shestakov, A. Theoretical Prediction of S−H Bond Rupture in Methanethiol Upon Interaction with Gold. *J. Phys. Chem. A* **2012**, *116*, 7686−7693.
(27) Olmos-Asar, J. A.; Rapallo, A.; Mariscal, M. M. Development of a Semiempirical Potential for Simulations of Thiol−Gold Interfaces. Application to Thiol-Protected Gold Nanoparticles. *Phys. Chem. Chem. Phys.* **2011**, *13*, 6500−6506.
(28) Zhou, J.-G.; Williams, Q. L. How Does an External Electrical Field Affect Adsorption Patterns of Thiol and Thiolate on the Gold Substrate? *J. Phys.: Condens. Matter* **2009**, *21*, 055008.
(29) Maksymovych, P.; Sorescu, D. C.; Yates, J. T. Methanethiolate Adsorption Site on Au(111): A Combined STM/DFT Study at the Single-Molecule Level. *J. Phys. Chem. B* **2006**, *110*, 21161−21167.
(30) Cometto, F. P.; Paredes-Olivera, P.; Macagno, V. A.; Patrito, E. M. Density Functional Theory Study of the Adsorption of Alkanethiols on Cu(111), Ag(111), and Au(111) in the Low and High Coverage Regimes. *J. Phys. Chem. B* **2005**, *109*, 21737−21748.
(31) Vélez, P.; Dassie, S. A.; Leiva, E. P. M. Role of Metal Contacts in the Mechanical Properties of Molecular Nanojunctions: Comparative Ab Initio Study of Au/1,8-octanedithiol and Au/4,4-bipyridine. *Phys. Rev. B: Condens. Matter Mater. Phys.* **2010**, *81*, 235435.
(32) Qi, Y.; Qin, J.; Zhang, G.; Zhang, T. Breaking Mechanism of Single Molecular Junctions Formed by Octanedithiol Molecules and Au Electrodes. *J. Am. Chem. Soc.* **2009**, *131*, 16418−16422.
(33) Bourg, M.-C.; Badia, A.; Lennox, R. B. Gold−Sulfur Bonding in 2D and 3D Self-Assembled Monolayers: XPS Characterization. *J. Phys. Chem. B* **2000**, *104*, 6562−6567.
(34) Azzam, W.; Wehner, B. I.; Fischer, R. A.; Terfort, A.; Wöll, C. Bonding and Orientation in Self-Assembled Monolayers of Oligophenyldithiols on Au Substrates. *Langmuir* **2002**, *18*, 7766−7769.
(35) Duwez, A.-S. Exploiting Electron Spectroscopies to Probe the Structure and Organization of Self-Assembled Monolayers: A Review. *J. Electron Spectrosc.* **2004**, *134*, 97−138.
(36) Andreoni, W.; Curioni, A.; Grönbeck, H. Density Functional Theory Approach to Thiols and Disulfides on Gold: Au(111) Surface and Clusters. *Int. J. Quantum Chem.* **2000**, *80*, 598−608.
(37) Franzen, S. Density Functional Calculation of a Potential Energy Surface for Alkane Thiols on Au(1 1 1) as Function of Alkane Chain Length. *Chem. Phys. Lett.* **2003**, *381*, 315−321.
(38) Mulliken, R. S. Electronic Population Analysis on LCAO-MO Molecular Wave Functions. II. Overlap Populations, Bond Orders, and Covalent Bond Energies. *J. Chem. Phys.* **1955**, *23*, 1841−1846.
(39) Angelici, R. J.; Lazar, M. Isocyanide Ligands Adsorbed on Metal Surfaces: Applications in Catalysis, Nanochemistry, and Molecular Electronics. *Inorg. Chem.* **2008**, *47*, 9155−9165.
(40) Kim; Beebe, J. M.; Jun, Y.; Zhu, X.-Y.; Frisbie, C. D. Correlation Between HOMO Alignment and Contact Resistance in Molecular Junctions: Aromatic Thiols versus Aromatic Isocyanides. *J. Am. Chem. Soc.* **2006**, *128*, 4970−4971.
(41) Kiguchi, M.; Miura, S.; Hara, K.; Sawamura, M.; Murakoshi, K. Conductance of a Single Molecule Anchored by an Isocyanide Substituent to Gold Electrodes. *Appl. Phys. Lett.* **2006**, *89*, 213104−213104−3.
(42) Jiang, D.; Sumpter, B. G.; Dai, S. Structure and Bonding Between an Aryl Group and Metal Surfaces. *J. Am. Chem. Soc.* **2006**, *128*, 6030−6031.
(43) De la Llave, E.; Ricci, A.; Calvo, E. J.; Scherlis, D. A. Binding Between Carbon and the Au(111) Surface and What Makes It Different from the S−Au(111) Bond. *J. Phys. Chem. C* **2008**, *112*, 17611−17617.
(44) Ma, G.; Shen, X.; Sun, L.; Zhang, R.; Wei, P.; Sanvito, S.; Hou, S. Low-bias Conductance of Single Benzene Molecules Contacted by Direct Au−C and Pt−C Bonds. *Nanotechnology* **2010**, *21*, 495202.
(45) Nykänen, L.; Häkkinen, H.; Honkala, K. Computational Study of Linear Carbon Chains on Gold and Silver Surfaces. *Carbon* **2012**, *50*, 2752−2763.
(46) Cheng, Z.-L.; Skouta, R.; Vazquez, H.; Widawsky, J. R.; Schneebeli, S.; Chen, W.; Hybertsen, M. S.; Breslow, R.; Venkataraman, L. In Situ Formation of Highly Conducting Covalent Au-C Contacts for Single-Molecule Junctions. *Nat. Nanotechnol.* **2011**, *6*, 353−357.
(47) Chen, W.; Widawsky, J. R.; Vázquez, H.; Schneebeli, S. T.; Hybertsen, M. S.; Breslow, R.; Venkataraman, L. Highly Conducting π-Conjugated Molecular Junctions Covalently Bonded to Gold Electrodes. *J. Am. Chem. Soc.* **2011**, *133*, 17160−17163.
(48) Medeiros, P. V. C.; Gueorguiev, G. K.; Stafström, S. Benzene, Coronene, and Circumcoronene Adsorbed on Gold, and a Gold Cluster Adsorbed on Graphene: Structural and Electronic Properties. *Phys. Rev. B: Condens. Matter Mater. Phys.* **2012**, *85*, 205423.
(49) Aradhya, S. V.; Frei, M.; Hybertsen, M. S.; Venkataraman, L. Van der Waals Interactions at Metal/Organic Interfaces at the Single-molecule Level. *Nat. Mater.* **2012**, *11*, 872−876.
(50) Paz, S. A.; Michoff, M. E. Z.; Negre, C. F. A.; Olmos-Asar, J. A.; Mariscal, M. M.; Sánchez, C. G.; Leiva, E. P. M. Anchoring Sites to the

STM Tip Can Explain Multiple Peaks in Single Molecule Conductance Histograms. *Phys. Chem. Chem. Phys.* **2013**, *15*, 1526−1531.
(51) Stokbro, K.; Taylor, J.; Brandbyge, M.; Mozos, J.-L.; Ordejón, P. Theoretical Study of the Nonlinear Conductance of Di-thiol Benzene Coupled to Au(111) Surfaces via Thiol and Thiolate Bonds. *Comput. Mater. Sci.* **2003**, *27*, 151−160.
(52) Paulsson, M.; Datta, S. Thermoelectric Effect in Molecular Electronics. *Phys. Rev. B: Condens. Matter Mater. Phys.* **2003**, *67*, 241403.